Optimal Design of Catenoidal Sonotrode for Ultrasonic Welding Process

Abdulhaqq A. Hamid * and Mohammed Najeeb Abdullah

Department of Mechanical Engineering, University of Mosul, Mosul, Iraq
Email: abdulhaqqhamid@uomosul.edu.iq (A.A.H.); moh_77@uomosul.edu.iq (M.N.A.)
*Corresponding author

***Abstract*—The Ultrasonic Welding (USW) process is mainly based on the design of the horn to ensure that it vibrates in the longitudinal position to achieve a proper welding process, and the best design of the horn is based on obtaining the largest possible amplitude during the longitudinal vibration. In the current study, the model and harmonic analysis were performed using the ANSYS/r21 program according to the response surface methodology matrix obtained from the software program, the design was optimized using the visual basic program, and the best horn design was found to provide the largest possible vibration amplitude. The findings demonstrate that the sonotrode can reach a maximum amplitude of 52.345 microns. And, the sonotrode's output face exhibits the highest longitudinal wave separation of 83.3% and the best uniformity of displacement amplitude when it comes to welding.**

***Keywords*—ultrasonic welding, catenoid sonotrode modal analysis, harmonic analysis, design optimization, response surface methodology**

I. Introduction

Welding is a vital process used across various industries to join similar and dissimilar materials and to create essential products and structures. However, traditional welding methods, such as arc welding, resistance welding, gas welding, and so on, often result in emissions of harmful fumes, high energy consumption, and significant waste generation. In response to environmental concerns and the need for more sustainable practices, clean welding technology has emerged as a promising solution. Clean welding technology refers to advanced welding techniques and processes that aim to minimize the environmental impact of welding operations. These technologies are designed to reduce emissions, energy consumption, and waste generation while maintaining high-quality welds [1].

Recently, even in the field of welding technology, clean technology has grown to be a significant study topic. The USW technique is being developed as a substitute for the traditional soldering process because the latter cannot be employed due to its toxicity. The former technique can fuse metal at its welds quickly, is safe for electrical use, and operates at room temperature. Additionally, the cost is inexpensive and the welding procedure is rather straightforward. Interfacial and intermolecular contacts generate heat during USW. The specimens are rubbed against one another while the horn pressure is applied during a standard USW procedure. As a result, at the joint interface, plastic deformation and metallurgical reaction are produced, which, when combined with thermal and ultrasonic softening, produce permanent bonding. This technique is safe for electrical use and operates at room temperature. Additionally, the cost is inexpensive and the welding procedure is rather straightforward. Ultrasonic frequency is the term used to describe the frequency range between 20 kHz and several gigahertz. When welding, high frequency ultrasonic vibration helps to facilitate the acoustic softening of materials. It functions on a similar principle to thermal softening. It is based on high-frequency vibrations, usually in the range of 20 to 70 kHz and small amplitude (10 to 250 μm) [2]. Fig. 1 shows a standard USW apparatus. The vibration and consolidation phases make up the two major stages of the USW process. Through the sonotrode, a vibration amplitude and welding force are applied to the components to be welded during the vibration period. An artificial surface asperity at the welding interface called an energy director is put there to encourage heat generation and prevent excessive bulk heating [3]. Before applying ultrasonic power during a typical ultrasonic welding cycle, the sonotrode is placed on the components that need to be welded. The top portion, which is the part facing the sonotrode, starts to vibrate in the direction of the sonotrode motion, causing a relative motion between the surfaces at the interface (rubbing motion) [4]. However, traditional welding methods, such as arc welding, resistance welding, gas welding, and so on, often result in emissions of harmful fumes, high energy consumption, and significant waste generation [5, 6].

Nad [7] designed sonotrodes for use in USW techniques. He examined the dynamic characteristics of several sonotrode shapes, including exponential, tapered, and cylindrical. Using the finite element technique, the impact of sonotrode dimensions on natural frequencies and mode shape is examined. The significance of correct sonotrode shape design is emphasized.

For the purpose to determine the ideal ultrasonic welding process parameters and obtain high welding

Manuscript received January 21, 2024; revised April 2, 2024; accepted April 8, 2024; published June 21, 2024.

strength, Taguchi and ANOVA techniques were used in [8]. The body of the power case is constructed of plastic for welding. Amplitude is the most important factor affecting welding strength; welding pressure, hold time, and trigger position come next. The optimal welding pressure, hold time, and operating position for the ultrasonic welding process were 115 kPa, 0.4 s, and 69.95 mm, respectively.

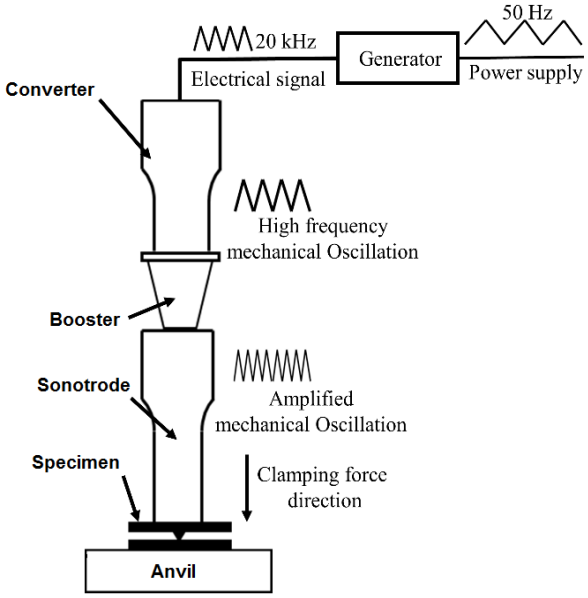

Fig. 1. The basic parts of ultrasonic welding apparatus [9].

Grabalosa *et al.* [9] illustrated how minute changes in size or shape caused by wear or cracks have a significant impact on a sonotrode's dynamic performance and how a sonotrode needs to be built correctly to guarantee that its performance respects machine and process requirements. It has been detailed how to use a graded sonotrode effectively for ultrasonic modulation. It was found that the length of the sonotrode point has an inverse relationship with the frequency of longitudinal vibration. The shorter tip length results in a higher sonotrode vibration frequency even though the longitudinal vibration mode is still generated.

Nguyen *et al.* [10] offered a method for obtaining uniform amplitudes in the sonotrode's working region. The aluminum alloy 7075 and stepped broad blade with a working frequency of 15 kHz were utilized to assess the amplitude distribution on the surface of the sonotrode 250×34 mm^2 using the finite element method. The sonotrode's shape can be changed to attain capacitance stability. It is discovered that the magnitude is high in the center and low on either side. To accomplish uniformity of amplitude extension, Steps are added to the input surface and two necks are added on either side to change the shape of the sonotrode based on this amplitude distribution.

Afshari and Arezoo [11] suggested a two-step process for optimizing wide sonotrode topology. In order to achieve a similar value for the longitudinal natural frequency, they designed wide sonotrodes. The frequency of operation of the transducer-booster causes the output face of the sonotrodes to vibrate uniformly.

Kumar *et al.* [12] examined a broad, grooved sonotrode. sixteen distinct experiments were made using the full factorial method. to measure the sonotrode's vibration amplitude and divide its wavelength in half in order to investigate the effects of slot position and dimensions.

Singha *et al.* [13], employed ANSYS software with finite elements to conduct a modal analysis of two different, somewhat difficult-to-manufacture horn profiles: steeped and exponential. The two aluminum and titanium profiles mentioned above have been considered in terms of their mode shape and inherent frequencies. The findings show that titanium alloy produces a higher natural frequency for all six modes in a stepped profile, but aluminum horn produces a higher natural frequency in the case of an exponential profile.

Kothuru *et al*. [14] increased the weld length on the weld bed surface with appropriate uniform amplitudes, an ultrasonic sonotrode is designed. At large weld lengths, the sonotrode design presents a significant challenge in achieving uniform amplitudes. In this instance, rectangular A sonotrode featuring multiple slots is engineered through theoretical computations and numerical analysis aimed at achieving the highest feasible weld lengths with consistent amplitudes at a predetermined operating frequency. The actual resonating frequency and amplitude distribution of the sonotrode are analyzed using the finite element method, yielding a maximum weld length of 400 mm at a frequency of 15 kHz with three slots.

The cost function of using USW can vary depending on several factors, including the specific application, materials being welded, equipment costs, labor costs, and maintenance and repair expenses. By well considering these factors and conducting a detailed analysis, it can develop a comprehensive cost function for using ultrasonic welding in your specific application [4].

The cost of USW is very low compared to traditional welding, as we do not need welding wire, and it is also an environmentally friendly welding process. Because of that metal welding requires less energy than ultrasonic plastic welding, it makes sense to build an instrument with a high amplification capacity to guarantee that a significant amount of energy is transferred to the work area with the least amount of loss. Additionally, manufacturing accuracy and productivity are guaranteed when the USW tool is designed with a modern approach. This research will concentrate on the design and advancement of this kind of USW tool because there hasn't been much done to improve catenoid -type welding tools [4, 5].

II. Material and Methods

The sonotrode was created as a half-wave resonator, and Aluminum Alloy AA6351 was employed to achieve superior strength and acoustic properties. Material characteristics are displayed in Table I. In this configuration, the ultrasonic metal welder was powered at a constant frequency of 20 kHz. The sonotrode length that would achieve resonance at 20 kHz and produce the highest amplitude at the sonotrode tip was determined using the equation of vibration and Fig. 2 shows the proposed welding area.

TABLE I. PROPERTIES OF ALUMINUM ALLOY AA 6351

Property	Value
Density (ρ)	2.74×10^3 kg/m^3
Youngs modulus (E)	74.5 GPa
Poisson's ratio (μ)	0.33

The suggested procedure for the theoretical and numerical analysis of the sonotrode is shown in Fig. 3 [15]. In order to ensure the wave's amplification and gain in amplitude, the length of the catenoidal sontrode, which is equal to half of the wavelength of 130 mm was calculated. The welding area for the assumed sample, which has a diameter of 15 mm, was specified as shown in Fig. 4, and the input diameter area of the sonotrode—which is typically greater was assumed to be in contact with the work piece [16].

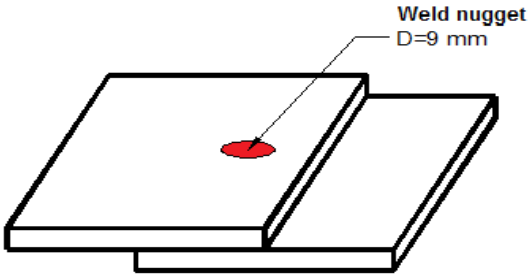

Fig. 2. Standard welding specimens with specified welding zone.

.

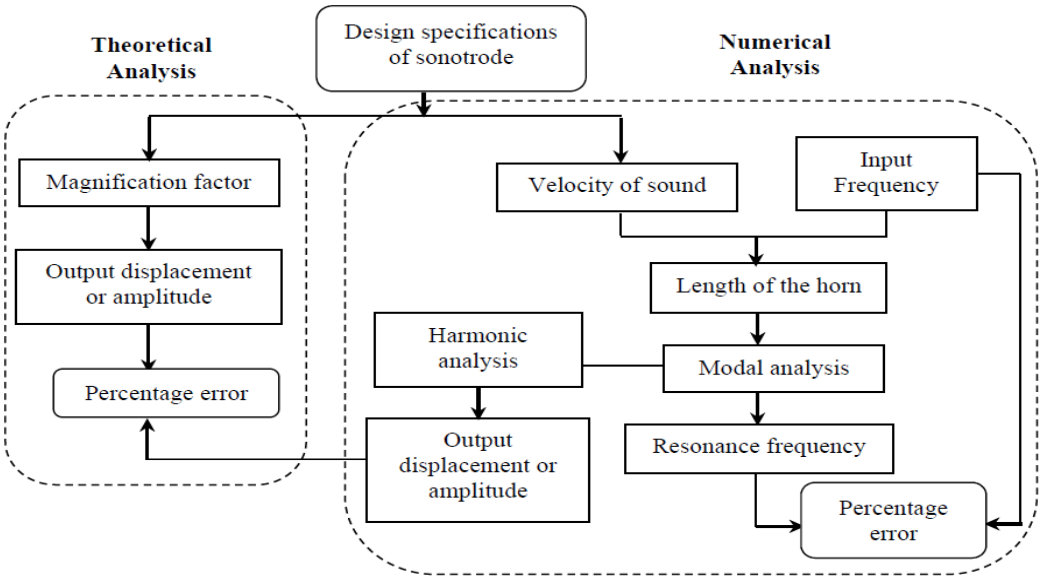

Fig. 3. Diagram showing the outlining of the theoretical and numerical analysis methodology [15].

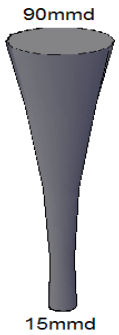

Fig. 4. Dimensions of catenoidal sonotrode proposed in this study.

The choice of the appropriate resonance frequency and resonant wavelength is crucial in the construction of solid sonotrode. The natural frequency of the ultrasonic sonotrode is determined analytically by solving the one-dimensional wave equation, which is influenced by the sonotrode's height Eq. (1).

$$\lambda = \frac{c}{f} = \frac{1}{f} \times \sqrt{\frac{E}{\rho}} = 2h \qquad (1)$$

Thus, $c = \sqrt{\frac{E}{\rho}} = 5215$ m/s, where λ is the wavelength of vibration (μm), c is the velocity of sound (m/s), h is the height of catenoidal sonotrode, h =130 mm, f is the vibration frequency (Hz), $and\ E$ is the young's modulus of sonotrode material (GPa).

III. RESULTS AND DISCUSSION

A. Modal and Harmonic Analysis

A finite element analysis is carried out following the modeling of the cleft mass sonotrode with the aforementioned dimensions. The model analysis's findings indicate that the sonotrode's face is flatter and has torsional, flexural, and longitudinal vibrations. As shown in Table II and Fig. 5.

TABLE II. NATURAL FREQUENCY MODES

Model Type	Natural Frequency (Hz)
Longitudinal mode	19010
Flexural mode	15593
Torsional mode	13789

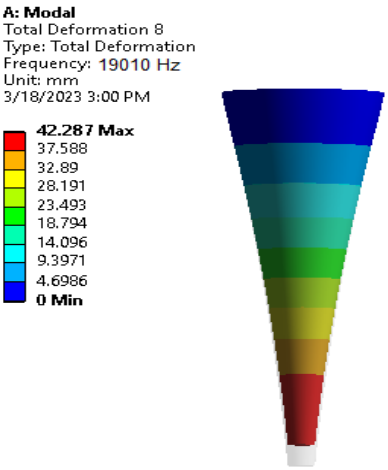

(a)

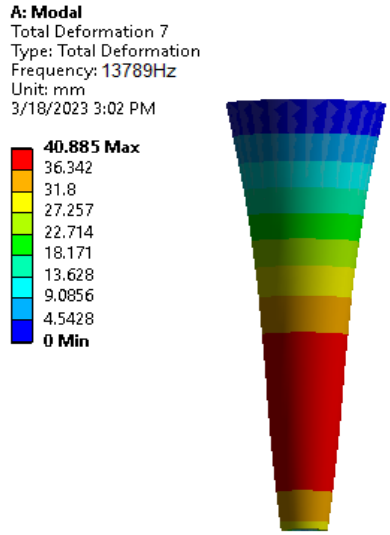

(b)

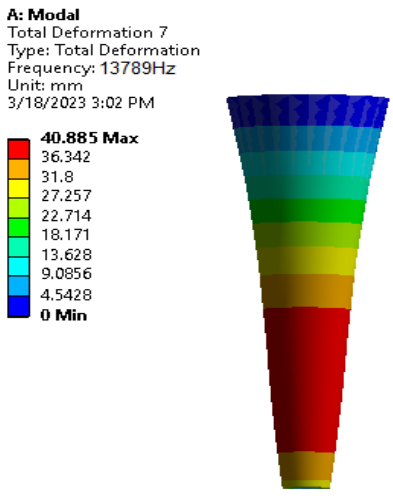

(c)

Fig. 5. Natural frequency for sonotrode; (a) Longitudinal mode, (b) Flexural mode, and (c) Torsional mode.

Then, using harmonic analysis, the displacement and stresses experienced by the sonotrode within the designated frequency range are ascertained. According to the harmonic analysis, the displacement amplitude at the sonotrode's output face is 47.4 μm as shown in Fig. 6.

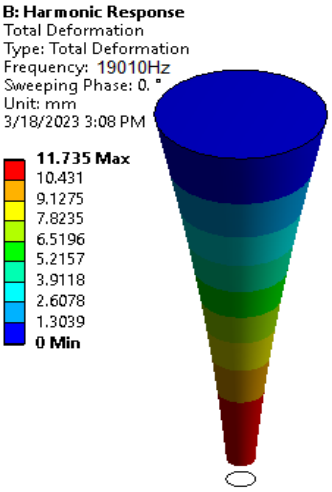

Fig. 6. Harmonic response of sonotrode.

B. Optimization of Catenoidal Sonotrode

The Response Surface Methodology as a statistical technique has recently become more critical for optimizing welding processes and minimizing costs by efficiently exploring the relationship between variables and responses, making it indispensable for modern scientific inquiry and industrial practice [17, 18]. The design of the experiment was used in this part to systematically investigate the effects of the design parameters (Y1, Y2) while taking into account their interdependence. These regression equations' coefficients of determination exhibit strong enough correlations to serve as objective functions (see Fig. 7 and Table III).

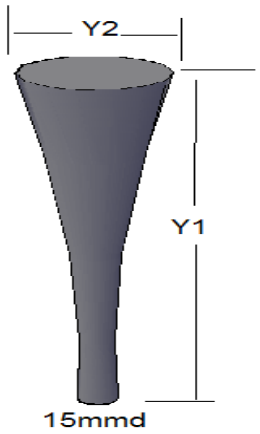

Fig. 7. Variables (dimensions) of sonotrode.

TABLE III. DISPLAYS DESIGN FACTORS AND THEIR LEVELS

Design variable	Levels (mm)	
Y1	130	140
Y2	80	100

A face-centered central composite design of trials is used to produce a variety of design variable combinations [19]. Based on response surface theory, which requires 13 responses to two variables to form an

equation representing the expected response to these variables, 13 different combinations of design variables are considered for the acoustic assessments of catenoidal sonotrodes. For a given catenoidal sonotrode dimension and machine frequency, harmonic analysis is used to determine the vibrational amplitude at the output face of the sonotrode, and the same amplitude is taken into consideration for insertion. The displacement amplitude derived from harmonic analysis is shown in Table IV for a range of design parameter combinations.

TABLE IV. HARMONIC ANALYSIS RESULTS FOR DIFFERENT COMBINATIONS OF THE DESIGN VARIABLES

No.	Y1 (mm)	Y2 (mm)	Amplitude (μm)
1	135	90	48
2	140	90	47
3	140	80	48
4	135	90	48
5	135	100	50
6	130	90	51
7	130	80	52
8	130	100	49
9	135	90	48
10	135	80	49
11	135	90	48
12	140	100	46
13	135	90	47

A non-linear model for displacement amplitude is created using RSM and based on the findings of the FEA. It is given in Eq. (2) and Fig. 8 displays the response surface to demonstrate the relationship between design variables and response.

$$\text{Amplitude(micron)} = 414 - 3.61\,Y1 - 2.11\,Y2 + 0.0103\,Y1\times Y1 + 0.00759\,Y2\times Y2 + 0.0050\,Y1\times Y2 \quad (2)$$

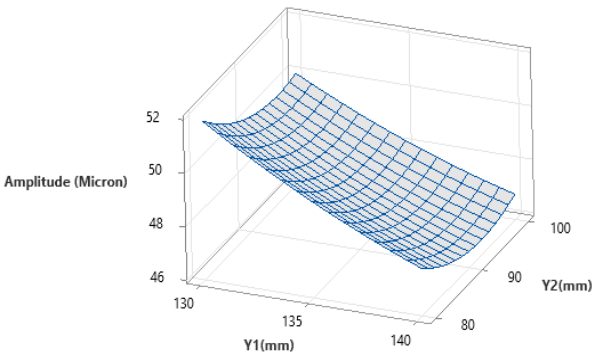

Fig. 8. Response surface between parameters and the resulting amplitude.

Fig. 9 indicates how each variable affects the relationship between the variables and response for each term in the non-linear equation. It is clear from the diagram that the variable Y1 has the greatest effect on the response, which is represented by the capacity, while the effect of the variable Y2 had a lesser effect on the capacity of the welding tool. The diagram below also shows the effect of each term of Eq. (2) on the response.

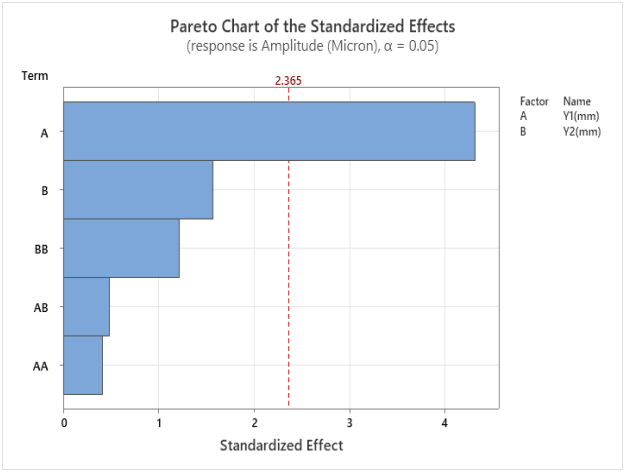

Fig. 9. Effect of variables according to each term of the non-linear equation.

The non-linear model developed for the vibration amplitude from RSM is applied. A Visual Basic (VB) program was utilized to optimize the catenoidal sonotrode's design. Eqs. (3) and (4) provide the constraints for the insertion process, while Eq. (2) provides the input fitness function. The Visual Basic program is used to optimize the design of the catenoidal sonotrode. The results of the VB program are shown in Table V. Using the Sequential Quadratic Programming (SQP) method, the optimal design parameters are found based on these regression models.;

$$130 \text{ mm} \le Y1 \le 140 \text{ mm} \quad (3)$$

$$80 \text{ mm} \le Y2 \le 100 \text{ mm} \quad (4)$$

TABLE V. CONVERGED VALUES OF DESIGN VARIABLES

Y1 (mm)	Y2 (mm)	Amplitude (Micron)
131	98.2	52.345

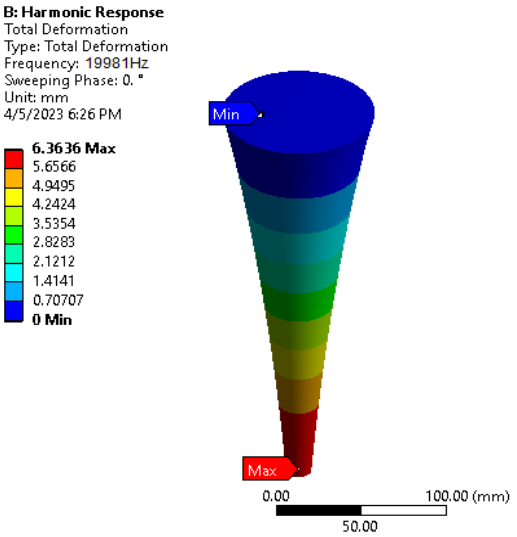

Fig. 10. Harmonic response of sonotrode.

A model and harmonic analysis are used to validate the best catenoidal sonotrode design that can be created with a VB program. Additionally, the results of the harmonic analysis of the best catenoidal sonotrode design are displayed in Fig. 10. The catenoidal sonotrode's free end, also referred to as the output face, experiences the largest amplitude along the longitudinal location of the vibration (19.799 kHz), which is 26.82 μm, as can be seen in the Fig. 10.

IV. Conclusions

In the current study, a quadratic mathematical model using RSM was developed. The upgraded RS model was paired further with the VB program to find the best design which led to maximizing strength. Moreover, it was concluded that the weld strength increases with the increase in capacitance because the increase in capacity gives more surface area for friction to work between surfaces that perform better bonding and increase weld strength. The sonotrode with the highest separation of the longitudinal wave used in welding of 1.598 μm for the torsional mode from the longitudinal mode and 4.366 μm for the flexural mode from the longitudinal mode—achieved a maximum amplitude of value of 52.345 μm. It also had the best uniformity of the displacement amplitude on the sonotrode's output face, at approximately 83.3%.

Conflict of Interest

The authors declare no conflict of interest.

Author Contributions

Abdulhaqq A. Hamid: Investigation, Methodology, Writing and Original Draft; Mohammed Najeeb Abdullah writing, Review, and Editing; all authors had approved the final version.

Acknowledgment

The authors would like to express our sincere gratitude to the Department of Mechanical Engineering, College of Engineering, Mosul University, Mosul–Iraq, for their invaluable support and guidance throughout the completion of this research paper. The depth of knowledge, encouragement, and resources provided by the department played a pivotal role in shaping the outcome of this study.

References

[1] X. M. Cheng, K. Yang, J. Wang, W. T. Xiao, and S. S. Huang, "Ultrasonic system and ultrasonic metal welding performance: A status review," *Journal of Manufacturing Processes*, vol. 84, pp. 1196–1216, December 2022. http://doi.org/10.1016/j.jmapro.2020.10.067

[2] Z. B. Zhang, X. D. Wang, Y. Luo, Z. Q. Zhang, and L. D. Wang, "Study on heating process of ultrasonic welding for thermoplastics," *J. Thermoplast. Compos. Mater*., vol. 23, no. 5, pp. 647–664, Sep. 2010. http://doi: 10.1177/0892705709356493

[3] Ultrasonic spray benefits sono-tek. [Online]. Available: https://www.sono-tek.com/ultrasoniccoating/ultrasonicspraybenefits/?gclid=Cj0KCQjwlahBhD7ARIsAM9tQKuF5QOkCyzOsJNeFf6opIDEc3hSxgaXPBtPvrS6uxnnz14U56c-kl0aAjKiEALw_wcB

[4] Summary of process advantages and disadvantages. [Online]. Available: https://msd.com.ua/new-developments-in-advanced-welding/summary-of-process-advantages-and-disadvantages/

[5] R. J. Jassim; H. M. Lieth, R. A. Sabur, and A. Alsahlani, "Influence of welding parameters on optimization of the tensile strength and peak temperature in AISI 1020 alloy joints welded by SAW," in *Proc. 4th International Conference on Materials Engineering and Science: Insight on the Current Research in Materials Engineering and Science*, November 17, 2022, vol. 2660, issue 1. doi: 10.1063/5.0107839

[6] S. J. Kadhim, R. K. A. Sabur, and A. B. K. Ali, "Application of different median filter algorithms for welding defects clarification in radiographic images," *University of Thi-Qar Journal for Engineering Sciences*, vol. 11, 2020.

[7] M. Nad, "Ultrasonic horn design for ultrasonic machining technologies," *Appl. Comput. Mech.*, vol. 4, Jun. 2010.

[8] C. C. Kuo, Q. Z. Tsai, D. Y. Li, Y. X. Lin, and W.-X. Chen, "Optimization of ultrasonic welding process parameters to enhance weld strength of 3C power cases using a design of experiments approach," *Polymers*, vol. 14, no. 12, p. 2388, Jun. 2022. doi: 10.3390/polym14122388

[9] J. Grabalosa, I. Ferrer, O. M. Romero, A. E. Zúñiga, X. Plantá, and F. Rivillas, "Assessing a stepped sonotrode in ultrasonic molding technology," *Journal of Materials Processing Technology*, vol. 229, 2016. doi: 10.1016/J.JMATPROTEC.2015.10.023

[10] T. H. Nguyen, Q. T. Quang, C. L. Tran, and H. L. Nguyen, "Investigation the amplitude uniformity on the surface of the wide-blade ultrasonic plastic welding horn," in *Proc. IOP Conf. Ser. Mater. Sci. Eng.*, Oct. 2017, vol. 241, no. 1, 012023. doi: 10.1088/1757-899X/241/1/012023

[11] M. Afshari and B. Arezoo, "Design of wide ultrasonic sonotrodes based on topology optimization," *Eng Optim*., pp. 1–21, 2021.

[12] R. D. Kumar, M. R. Rani, and S. Elangovan, "Design and analysis of slotted sonotrode for ultrasonic plastic welding," *Appl. Mech. Mater.: Trans. Tech. Publ.*, pp. 859–863, 2014.

[13] D. P. Singha, S. Mishra, and R. K. Porwalc, "Modal analysis of ultrasonic horn using finite element method," *Materials Today*, vol. 18, 2019.

[14] V. V. L. Kothuru, V. S. Sistla, I. H. Mohammed, and A. Jagana, "Design and numerical analysis of rectangular sonotrode for ultrasonic welding," *Trends in Sciences*, vol. 481, 2022.

[15] V. V. L. Kothuru, V. S. Sistla, I. H. Mohammed, and A. Jagana, "Design and numerical analysis of rectangular sonotrode for ultrasonic welding," *Trends Sci*., vol. 19, no. 11, 11, May 2022. doi: 10.48048/tis.2022.4215

[16] E. Kim, H. Jang, and D. Park, "Design of ultrasonic horn for slip-ring metal welding," *Adv. Mater. Res*., vol. 129–131, pp. 536–541, Aug. 2010. doi: 10.4028/www.scientific.net/AMR.129-131.536

[17] R. A. Sabur, M. Slobodyan, S. Chhalotre, and M. Verma, "Contact resistance prediction of zirconium joints welded by small scale resistance spot welding using ANN and RSM models," *Materials Today*, vol. 47, 2021. doi.org/10.1016/j.matpr.2021.04.431 2214-7853/ 2021

[18] R. A. Sabur, "Tensile strength prediction of aluminum alloys welded by FSW using response surface methodology—Comparative review," *Materials Today*, vol. 45, 2020. doi.org/10.1016/j.matpr.2020.12.1001 2214-7853/2021.

[19] J. C. Hung, Y. P. Tsai, and C. H. Hung, "Optimization of ultrasonic plastic welding horns on amplitude uniformity," *Front. Manuf. Des. Sci. II*, pp. 278–282, Jan. 2012. doi: 10.4028/www.scientific.net/AMM.121-126.278